ELSEVIER

Polymer 40 (1999) 1781–1789

polymer

Blends of new, all-aromatic liquid-crystalline polymers and poly(ethylene terephthalate)

L. Carpaneto[a,*], G. Lesage[a], R. Pisino[a], V. Trefiletti[b]

[a]*Dipartimento di Chimica e Chimica Industriale, Università di Genova, Via Dodecaneso 31, 16146 Genoa, Italy*
[b]*Istituto Studi Chimico Fisici di Macromolecole Sintetiche e Naturali – CNR, Via De Marini 6, 16149 Genoa, Italy*

Received 17 February 1998; accepted 1 May 1998

Abstract

Thermal, mechanical, dynamical mechanical and morphological investigations are reported of two series of blends of poly(ethylene terephthalate) (PET) with two nematogenic random polymers synthesized in our laboratory. The nucleant effect of low amounts of the liquid-crystalline component (LCP) is evidenced by thermal analysis for both polymers. At higher LCP contents this effect disappears but a new influence on the melting enthalpy of PET emerges, although at contents of the random polymer that are remarkably different for the two series of blends. The coupling of mechanical tests with a morphological study allowed elucidation of the reinforcing mechanism of one of the nematogenic polymers and the explanation of the discontinuity in the rise of Young's modulus shown by these blends.

Keywords: Aromatic liquid-crystalline polymers; Poly(ethylene terephthalate); Blends

1. Introduction

Polymer blends between conventional thermoplastics and liquid-crystalline polymers (LCPs) have attracted much interest during the last decade. Processing enhancements, together with the higher mechanical, physical and chemical properties obtained by blending, and the opportunity to obtain lower-cost materials compared with the pure LCPs, have focused efforts on the determination of polymer/LCP systems suitable for industrial exploitation [1–6]. Several parameters affect the final properties of products obtained by 'in situ' reinforced thermoplastics, with interphase adhesion and morphology of the dispersed LCP phase playing two of the most important roles. Both these aspects depend on the chemical nature of the two polymers, but it is also possible to affect them, at least to some extent, by varying the processing conditions [7–15].

One of the great drawbacks in technological application of thermotropic polymers is their high melting temperature, and many efforts have been dedicated to design polymers that exhibit a transition to a liquid-crystalline melt well below their decomposition temperature [16]. Recently, the insertion of 3,4′-substituted diaromatic monomers into the macromolecular chain proved to be an alternative route to obtain processable thermotropic polymers [17–19]. As a consequence of our work on these monomers and the all-aromatic linear polymers (having accessible melting temperatures) derived from them [20–23], we decided to test two polymers showing thermotropic behaviour as components of blends with poly(ethylene terephthalate) (PET). In this paper, we report syntheses that have not been described previously in the literature and the results of calorimetric, dynamical mechanical, morphological and mechanical analyses of PET/LCP blends of different composition.

2. Experimental

2.1. Characterization techniques

Proton nuclear magnetic resonance (^{1}H-n.m.r.) spectra of monomers and intermediates were obtained on a Varian Gemini 200 spectrometer (with tetramethylsilane as internal standard). All calorimetric measurements were carried out with a Perkin–Elmer DSC7 differential scanning calorimeter under dry nitrogen as purge gas; transition temperatures and enthalpies were determined with dedicated software. Optical observations were performed by using a

* Corresponding author. Tel.: +39-010-3538718; fax: +39-010-3536199; e-mail: carpanet@chimica.unige.it

0032-3861/99/$ - see front matter
PII: S0032-3861(98)00407-8

Reichert-Jung Polyvar Pol polarizing microscope and a Mettler FP 82 HT hot-stage connected to an FP 90 processor. The thermal stability of the polymers was investigated by a Perkin–Elmer TGS2 analyser (heating rate of 10°C min^{-1}, dry nitrogen atmosphere). A Polymer Laboratories Mk-III dynamical mechanical thermal analyser (in single cantilever mode, 1 Hz frequency, 2°C min^{-1} heating rate), a Leica Stereoscan 440 scanning electron microscope (20 kV accelerating voltage) and an Instron 5565 dynamometer (20 mm min^{-1} shaft translation speed) were also used to characterize unalloyed polymers and their blends.

2.2. Materials

N,*N*-dimethylformamide (DMF) (Aldrich, 99.8%), pyridine (Py) (Fluka, 99.8%) and diphenylchlorophosphate (DPCP) (Aldrich, 99.0%), were used as received; *p*-hydroxybenzoic acid (HBA) was recrystallized from water and 6-hydroxy-2-naphthoic acid (HNA) from water/ethanol (60/40 v/v).

2.3. Monomers

Two asymmetrical monomers were used in this work: 3-(4-hydroxyphenylthio)benzoic acid [4-(3-HPT)BA] and 4-(3-hydroxyphenoxy)benzoic acid [4-(3-HP)BA]. The synthetic routes followed to obtain both compounds are reported in the literature [19,22], the only difference being in the reactant used to cleave the methoxy group to obtain 4-(3-HP)BA (here hydroiodic acid was used instead of hydrobromic acid [19]).

2.3.1. Synthesis of 4-(3-HP)BA

4-(3-HP)BA was obtained by a two-step synthesis. A suitably modified Ulmann reaction [24,25] between 3-bromoanisole and 4-ethylhydroxybenzoate gave, after basic hydrolysis, the methoxylated precursor, 4-(3-methoxyphenoxy)benzoic acid; this intermediate was treated with hydroiodic acid to cleave the methoxy group and obtain the desired product.

2.3.2. Synthesis of 3-(4-HTP)BA

This monomer was obtained in a three-step reaction, involving preparation of the intermediate 3-(4-methoxyphenylthio)benzonitrile by an Ulmann reaction, successive hydrolysis of the intermediate to the corresponding carboxylic acid and finally demethoxylation by BBr_3 to give the hydroxyacid [22].

2.4. Polymer synthesis

Two random polymers, containing the asymmetric monomers, were chosen to study their blends with PET because of their nematogenicity and good reproducibility of measurable parameters such as glass transition and melting temperature of different preparative batches. Their structures are shown below.

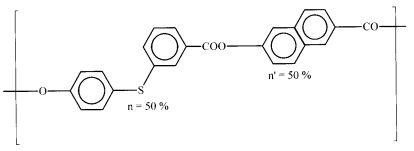

P1: 3-(4-HTP)BA / HNA 50/50 mol/mol

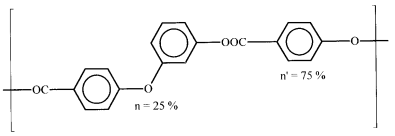

P2: 4-(3-HP)BA / HBA 25/75 mol/mol

The polymers were synthesized by direct condensation of hydroxyacids in the presence of DPCP and DMF in Py according to the method of Higashi [26].

Both resulting polymers were insoluble in specific solvents for polyesters and their inherent or intrinsic viscosity could not be determined, preventing an investigation on their molecular weight. As will be shown later, **P1** is totally amorphous whereas **P2**, in agreement with the literature, is somewhat crystalline [19]. Both polymers proved to be stable up to temperatures exceeding 440°C (temperature of 10% weight loss: 480°C for **P1** and 440°C for **P2**).

2.5. Preparation of blends

PET ($M_v = 19\,000$ g mol^{-1} as determined by viscometry, solvent: phenol/1,1,2,2-tetrachloroethane 40/60 w/w) was used as blend component. Samples were studied in the form of small bars obtained with a micro extruder designed to process small amounts of the polymers, of the order of 1–2 g. The cylindrical heated chamber of the extruder is 13 mm wide and 16 mm deep; the molten fluid was mixed in this chamber with a thin rod and compressed into the mould by means of a hand-controlled piston. **P1**/PET blends were extruded as bars of dimensions 25 mm × 6 mm × 1.8 mm, whereas **P2**/PET samples were obtained as 35 mm × 4 mm × 1 mm bars. The different mould used for the latter system was chosen in order to have specimens suitable for mechanical testing; the mechanical properties of **P1**/PET did not seem of practical interest because of the relatively low glass transition temperature (T_g) of the LCP component and its totally amorphous state.

During the experiments it was observed that mixing in the heated chamber of the extruder was rather poor, at least for the short processing times required to minimize decomposition effects. Therefore, to ensure good dispersion of the two polymers, PET was first dissolved in $CF_3COOH/CHCl_3$ (30/70 v/v) and the chosen amount of **P1** or **P2** was then added to the solution. Although neither of LCP component is

Table 1
Thermal parameters of **P1** and **P2**

		T_g (°C)	T_m (°C)	ΔH_m (kJ mol^{-1})
P1		100	—	—
P2	first scan	79	232.0	0.40
	second scan	80	231.9	0.15

soluble, they were finely scattered in PET after precipitation in methanol. The mixtures were then washed and dried under vacuum at 65°C for 24 h before processing.

3. Results and discussion

3.1. Differential scanning calorimetry (d.s.c.)

P1, **P2**, PET, four **P1**/PET and five **P2**/PET blend compositions were investigated. All samples underwent two heating cycles from 25 to 280°C at 20°C min^{-1} with a quench to room temperature (cooling rate $>$ 130°C min^{-1}) between runs; in some cases third heating runs were performed to confirm data obtained in previous scans. Results are reported in Tables 1-6.

Whereas **P1** in blends showed a pure glass transition, the thermal phenomena of **P2** were of modest magnitude and did not seem worth taking into account in the following discussion, with possibly one exception. Therefore, thermal parameters for the PET/**P2** blends must be considered as being due to PET only.

The T_g values of **P1** and PET/**P1** blends were totally reproducible in the first and second scans. For **P1** contents above 10%, both blend components showed their glass transition at a temperature substantially unaffected by the presence of the other polymer (Fig. 1). PET/**P2** blends exhibited only the T_g of PET and its profile was usually disturbed in the first d.s.c. run, whereas it could be determined clearly in the following scan. When present in low amount **P1** and **P2** affected the crystallization rate of PET: indeed, while all of the samples showed cold crystallization during the first d.s.c. run (i.e., as-extruded), only blends with a high content of LCP underwent the same phenomenon in the second scan [Fig. 2(c), Fig. 2(d)]. Therefore, however fast the cooling rate in the instrument, only an abrupt freezing of the blend such as that experienced in the mould could prevent PET from crystallizing in large amount when a sufficiently low content of **P1** or **P2** was present; otherwise crystals formed during cooling and prevented any dramatic rearrangement during the following heating scan [Fig. 2(a), Fig. 2(b)]. This behaviour is found in other PET/LCP blends and is not surprising in itself, with the liquid-crystalline polymer acting as a nucleant; blends containing higher amounts of LCP did not show this behaviour and cold crystallization appeared again in the second scans.

Table 2
Thermal parameters of PET

PET	T_g (°C)	T_{cc} (°C)	ΔH_{cc} (kJ mol^{-1})	T_m (°C)	ΔH_m (kJ mol^{-1})
First scan	75	141.0	3.8	254.0	9.9
Second scan	77	141.0	1.47	254.0	8.0

Table 3
Thermal parameters of PET/**P1** blends (first scan)

PET/**P1** (w/w)	T_{g1} (°C)	T_{g2} (°C)	T_{cc} (°C)	ΔH_{cc} (kJ mol^{-1})	T_m (°C)	ΔH_m (kJ mol^{-1})
90/10	82	—	135.4	1.4	254.1	9.2
70/30	76	102	134.0	4.8	255.1	11.5
50/50	78	101	146.6	6.8	250.0	9.5
30/70	77	99	139.6	6.2	250.9	8.8

The amount and nature of the LCP also played a role in the melting parameters. In second scans, the melting enthalpies (ΔH_m) of blends with an LCP content of up to 50 wt% were usually 1–2 kJ mol^{-1} lower than those detected in the first run. This can be explained by taking into account the strong flow fields experienced by the polymers during extrusion, which imposed an orientation on PET with a consequent increase in crystallinity; in second scans, when the orientation was lost because of melting, fewer crystals formed and the overall ΔH_m decreased. In PET/**P1** systems melting enthalpies recorded during the first scan increased until the LCP content reached 30% with no effect on the melting temperature (T_m), while PET/**P2** blends showed the same trend in enthalpy but also an effect on melting temperatures that reached unusually high values (260–261°C) for contents of 10 and 20% in random polymer. This latter result was probably due to stretching effects in PET chains that were sheared at the interface with **P2**, since the viscosity of this polymer, under processing conditions, was higher than that of **P1**. Also, phase adhesion with PET was better, as seen from scanning electron micrographs presented below. This might lead to the formation of PET crystals of higher thickness which melt at high temperature. In second d.s.c. runs, with the orientation erased, the melting temperatures of these samples were again comparable to that of pure PET. When the liquid crystal polymers were present in high amount (at least 70% for **P1** and 40% for **P2**), the melting enthalpy of PET increased as a measure of a somewhat higher degree of crystallinity of the matrix, while its melting temperature decreased to 242°C for

Table 4
Thermal parameters of PET/**P1** blends (second scan)

PET/**P1** (w/w)	T_{g1} (°C)	T_{cc} (°C)	ΔH_{cc} (kJ mol^{-1})	T_m (°C)	ΔH_m (kJ mol^{-1})
90/10	82	—	—	254.2	8.6
70/30	76	—	—	254.5	8.6
50/50	78	147.7	5.7	251.4	8.2
30/70	77	149.0	6.2	248.3	9.6

Table 5
Thermal parameters of PET/**P2** blends (first scan)

PET/**P2** (w/w)	T_g (°C)	T_{cc} (°C)	ΔH_{cc} (kJ mol^{-1})	T_m (°C)	ΔH_m (kJ mol^{-1})
99/1	77	123.0	3.0	255.0	9.4
90/10	nd	135.0	2.1	261.3	10.0
80/20	nd	131.5	2.7	260.1	11.3
70/30	77	129.5	5.8	255.3	9.8
60/40	66	128.7	6.2	255.2	11.3
30/70	nd	132.7	6.7	243.2	9.6
0/100	79	—	—	232.4	0.4

nd: Not determined because of rough profile.

Table 6
Thermal parameters of PET/**P2** blends (second scan)

PET/**P2** (w/w)	T_g (°C)	T_{cc} (°C)	ΔH_{cc} (kJ mol^{-1})	T_m (°C)	ΔH_m (kJ mol^{-}1)
99/1	79	—	—	255.0	8.2
90/10	82	—	—	256.2	7.9
80/20	80	—	—	256.2	8.3
70/30	78	—	—	254.2	8.4
60/40	77	128.2	5.0	253.0	11.0
30/70	72	133.6	6.8	242.0	10.6
0/100	—	—	—	231.9	0.2

contents of **P2** as high as 70%. Whereas the latter phenomenon can be associated with a dilution effect, some mechanism, different from orientation-induced crystallization, must be considered to explain the high values of ΔH_m recorded for the samples with high LCP content compared with samples having a lower LCP content, since these values were reproducible in second and third runs (Tables 5 and 6, concentrations in **P2** higher than 40 wt%). This observation might be connected to the extension of interfacial surfaces and was very evident in PET/**P2** blends, where there is strong adhesion between the two polymers. It can be supposed that when the interface area is large enough, i.e., for high contents of liquid crystalline polymer, its influence on crystallinity becomes detectable. A **P2** content of 40 wt% brought about an increment of ca. 3 kJ mol^{-1} with respect to ΔH_m of pure PET, reproducible in second and third scans. It is possible that, at least in this system, chemical effects play a key role in favouring the crystallization in PET. For instance, transesterification reactions, even if in small amount, could take place during extrusion at high temperature because of the residual catalyst in PET. These reactions would produce block copolymers between PET and **P2** which, by placing themselves at the interface, would favour phase dispersion and adhesion but could also induce a sort of register in neighbouring PET chains and help crystallization. Of course, a similar effect could also take place in **P2** and its crystallinity may not be negligible in this case, as previously supposed in examining d.s.c. results. Moreover, because of the broad melting profile of the liquid-crystal polymer, it could be easily confused as a tail of the melting peak of PET.

Unfortunately, we could not find direct proof of this hypothesis because, should block copolymers form, their chemical likeness with the parent polymers and their low amount would make it difficult to detect them.

3.2. Dynamic mechanical thermal analysis (d.m.t.a.)

D.m.t.a. was performed on all samples except **P1** in two heating cycles up to 200°C, with a free cooling to room temperature between cycles. **P1** underwent a single scan because of an abrupt fall in modulus following its T_g and resultant deformation of the bar.

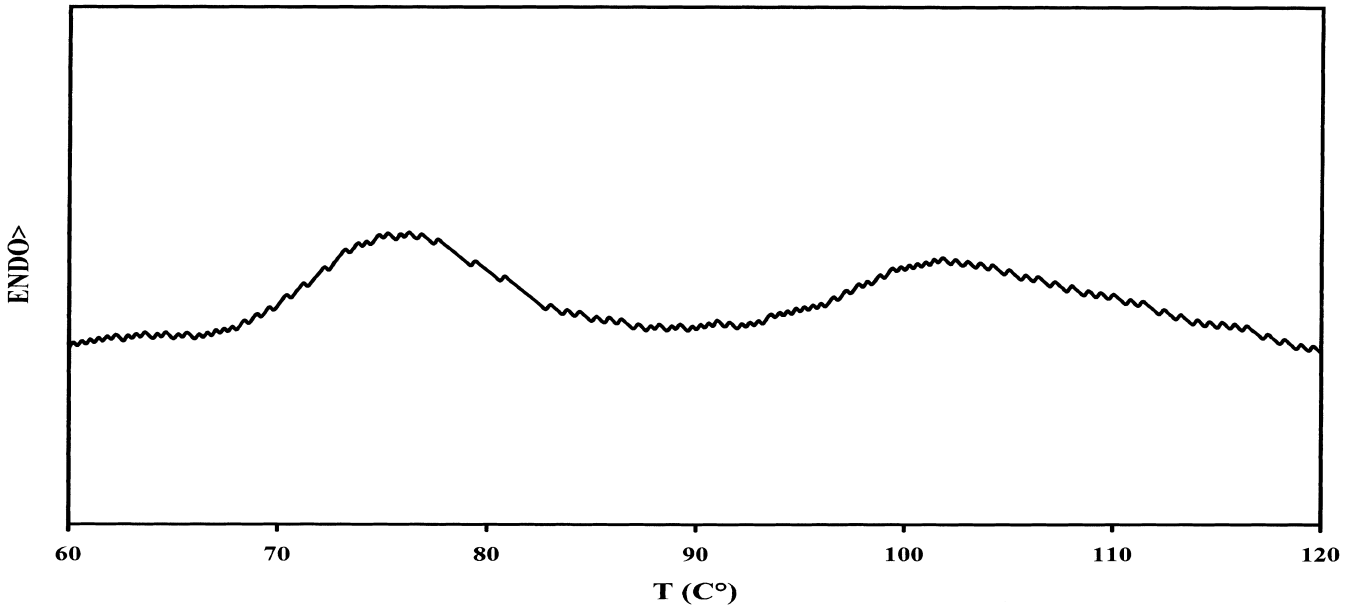

Fig. 1. D.s.c. trace of glass transitions in the PET/**P1** 70/30 w/w blend (at about 73 and 100°C for the PET and **P1** components, respectively).

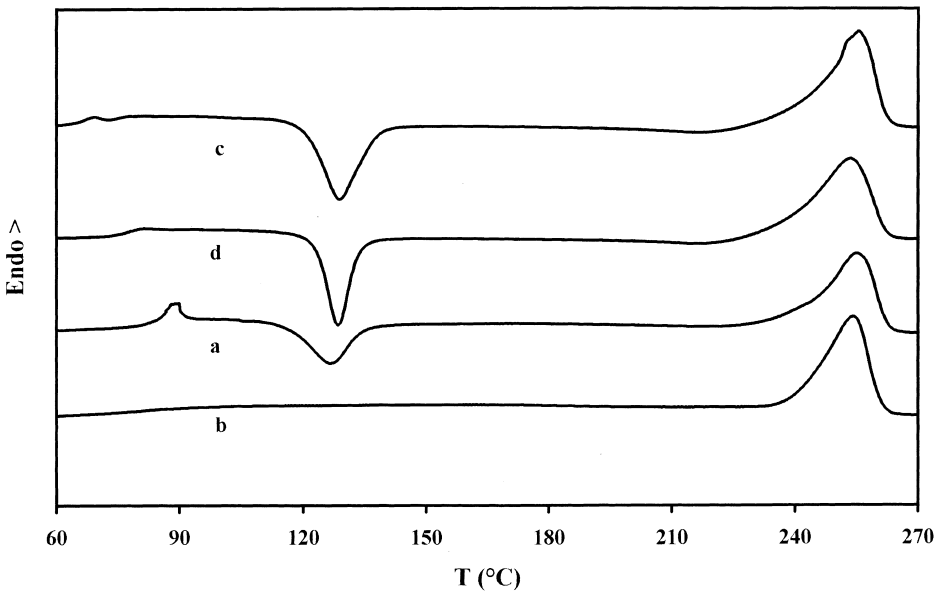

Fig. 2. (a) First and (b) second heating runs on PET/**P2** 90/10 w/w blend; (c) first and (d) second heating runs on PET/**P2** 60/40 w/w blend.

The damping parameter (tan δ) trace of pure PET shows a narrow and well-defined peak at 80°C, followed by a smaller one around 115°C due to cold crystallization [Fig. 3(a)]. In the second scan PET showed only one peak of much lower magnitude spanning over quite a broad temperature range (80–130°C), as shown in Fig. 3(b).

P1 presented a peak of tan δ of remarkable intensity at 105°C, in good accordance with d.s.c. results, while at higher temperature, as already mentioned, the specimen bar deformed and tended to flow. **P2**, by contrast, had a low tan δ peak at about 80°C and the trace raised steadily with temperature, a behaviour that was well reproduced in second scans.

PET/**P1** traces showed two marked tan δ peaks [Fig. 3(c)] and in the second scan, because of the highly crystallized PET matrix, only a smaller tan δ peak at about the same temperature as that of **P1** which must be considered as due to the overlapping of PET and **P1** signals [Fig. 3(d)]. The situation was different for systems containing **P2**, whose glass transition temperature is only a few degrees higher than that of PET, which exhibited a tan δ signal of low magnitude. Cold crystallization of the matrix made interpretation of these traces rather difficult, because it overlapped the rising signal due to **P2**, which appeared as a shoulder of the main peak that became more and more pronounced as the content in random polymer increased [Fig. 4(a), Fig. 4(b)]. Second scans were performed on systems that were highly crystallized because of the long annealing undergone by PET during the first cycle and therefore also in second scans of blends containing **P2**, only one peak was

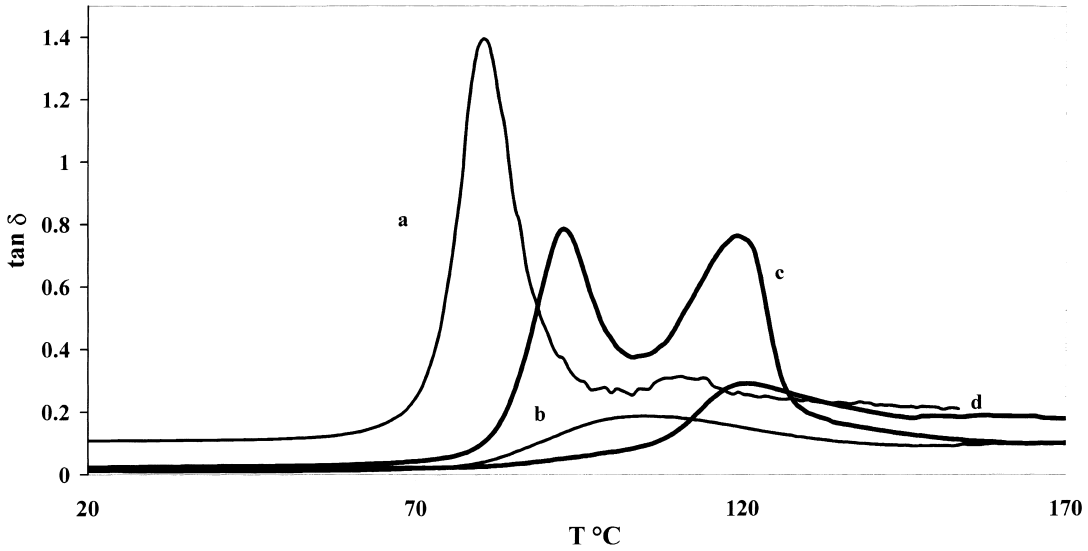

Fig. 3. D.m.t.a. traces of tan δ (a and c, first runs; b and d, second runs) for pure PET (a,b) and for the PET/**P1** 70/30 w/w blend (c,d).

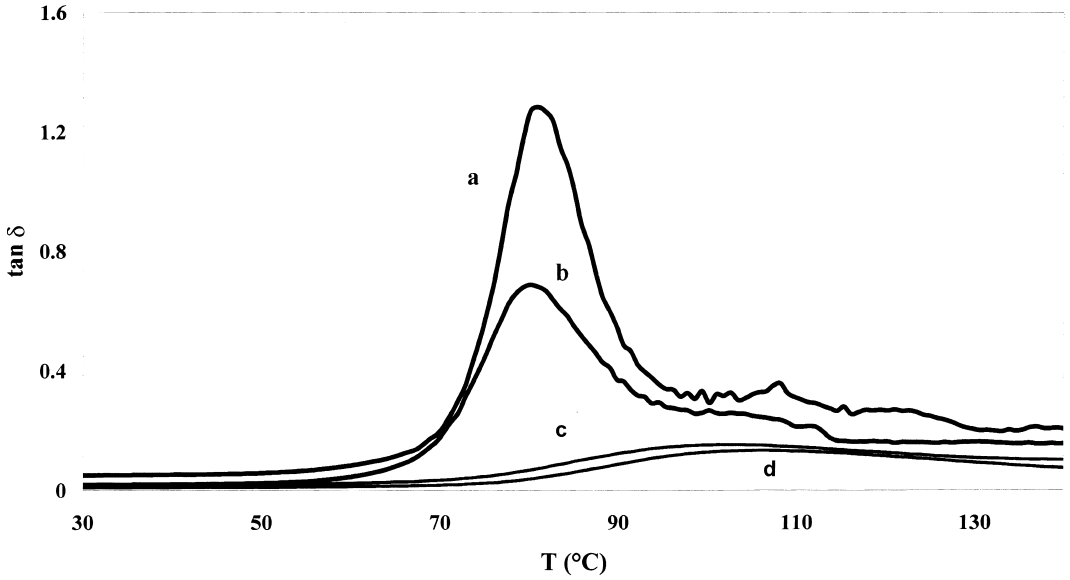

Fig. 4. D.m.t.a. traces of tan δ (a and b, first scans; c and d, second scans) for 80/20 w/w (a,c) and 60/40 w/w (b,d) PET/**P2** blends.

detectable. In this case, however, it seemed to shift towards lower temperatures with decreasing PET content. This fact must be attributed to a variation in the peak shape rather than to some miscibility of the two components, which should be more segregated than in first scans because of the crystallization of PET [Fig. 4(c), Fig. 4(d)].

3.3. Mechanical properties analysis

This analysis was not intended to give absolute values but only a comparison between PET and its blends with **P2** to test the possible reinforcing action on the thermoplastic by the LCP. It must be remembered that both the geometry of the specimens and their low number (approximately eight for any composition) do not provide a fully reliable characterization.

Three parameters were determined: Young's modulus, stress and strain at break. All five blends were tested in addition to pure PET; however, it was impossible to determine the mechanical properties of pure **P2** since sample bars cracked during clamping.

As can be seen in Table 7, all values except strain at break

Table 7
Mechanical properties of PET/**P2** blends

PET/**P2** (w/w)	Young's modulus (GPa)	σ_{break} (MPa)	ϵ_{break} (%)
100/0	0.97	26	181
90/10	1.08	31	181
80/20	1.25	35	52
70/30	1.20	40	9
60/40	1.21	28	6
30/70	1.34	45	7
0/100	nd	nd	nd

nd: Not determined.

are improved by increasing the content of **P2** with respect to pure PET. Passing from 10 to 20% of **P2** in the blend, Young's modulus showed an increase from about 1 to 1.25 GPa and then remained almost unchanged until **P2** became the main component. Even though the highest σ_{ba} and modulus values were reached for specimens containing 70% of the LCP, their behaviour was extremely fragile, whereas the 80/20 blend seemed to reach a good compromise between a relatively high modulus and ductility. When the amount of **P2** rose to 30%, the samples did not exhibit uniform fracture behaviour; several samples were brittle but others still showed some ductility. This blend, which marks the passage from ductility to brittleness, is probably very sensitive to small changes in local composition and all of the mechanical data reported for this composition must be considered unrepresentative.

It must be noted that the overall increase in Young's modulus was moderate up to the maximum content of **P2** that could be reached ($\approx$ 0.4 GPa) and this can be attributed to **P2** acting as a dispersed particulate reinforcing agent, even though its modulus could not be estimated.

3.4. Morphology

Morphological analysis was performed after fracture of specimens in liquid nitrogen and, for blends of PET with **P2**, also for specimens broken during mechanical testing. All blends showed a clear biphasic nature and only when the LCP was present in very low amount (1%) was it difficult to detect its presence. Fig. 5(A), a micrograph of the PET/**P1** 90/10 blend, shows the fibrous nature of the domains of the LCP. Increasing the content of **P1** in the blend (30%) brought about a more homogeneous distribution of LCP domains, as illustrated in Fig. 5(B), where also is evident the fibrillar morphology of the polymer due to its low

viscosity at processing temperature. The holes in the PET matrix, left after the pull-out of fibrils during failure, prove that adhesion between the two phases is not outstanding; on the other hand, it must be considered that the tensile modulus of **P1** was not determined and could well account for high pulling strengths acting on the matrix. For higher amounts of random polymer there was a gradual change in morphology which, at 70% of LCP, was difficult to interpret; phase inversion may have occurred, even though this could not be easily evidenced because of the fibrous nature of **P1**.

The morphology of **P2** in blends with PET showed no evident difference with varying blend composition. Spherical droplets of small diameter (≈ 1–$3\ \mu$m) could be found uniformly scattered in the sample even at low concentrations and they always showed good adhesion to the matrix. Their fracture did not present a fibrous nature but rather a sort of tree-ring morphology [Fig. 6(A)]. Another view of the fractured droplets in a blend with 40% **P2** is reported in Fig. 6(B) where it can be noted that, although in this case the content of **P2** is quite high, only the droplet density and not their dimensions grow, and incipient coalescence can be observed. A fibrillar morphology could be observed only near the border of some bars with a low content of **P2**, although the shape ratio could not be determined. In specimens with high **P2** content (70%), PET seems to be segregated in islands of large dimensions (tens of μm) as can be observed in Fig. 7, with a morphology

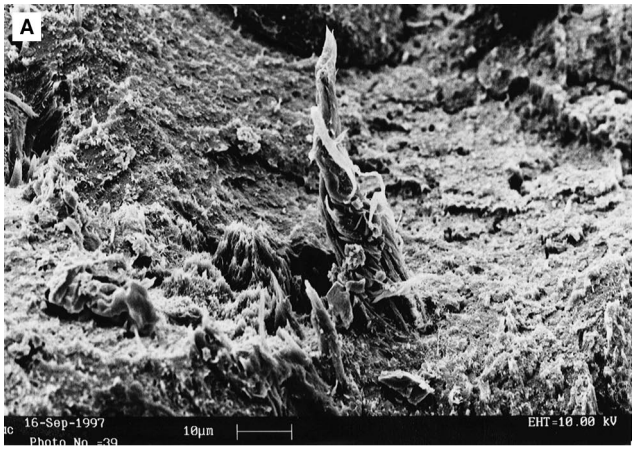

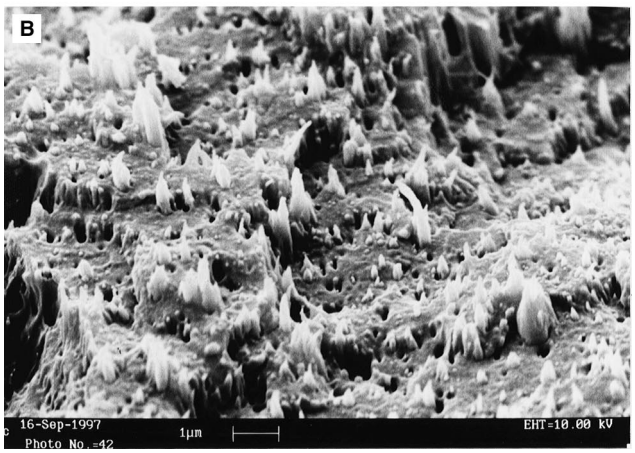

Fig. 5. Micrographs of: (A) PET/**P1** 90/10 w/w blend, showing the fibrous nature of random polymer **P1**; (B) PET/**P1** 70/30 w/w blend, showing finely scattered **P1** fibrils.

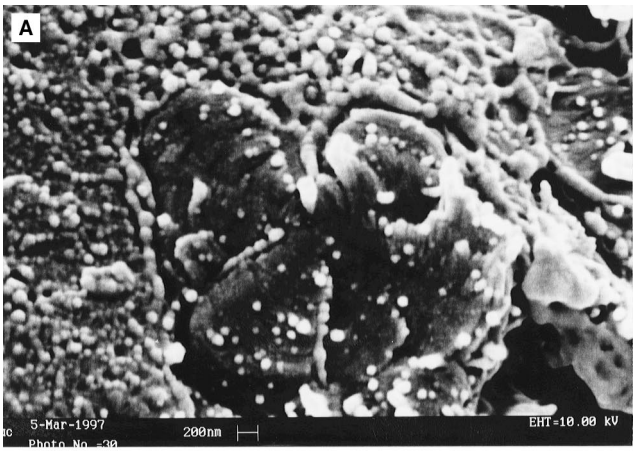

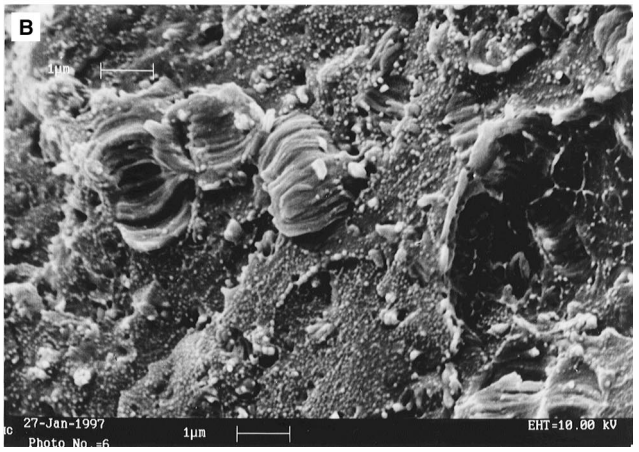

Fig. 6. Micrographs of: (A) PET/**P2** 90/10 w/w blend, showing detail of the 'tree-ring' morphology of the droplet; (B) PET/**P2** 60/40 w/w blend, showing that **P2** droplets are always of the same dimensions, although more densely scattered.

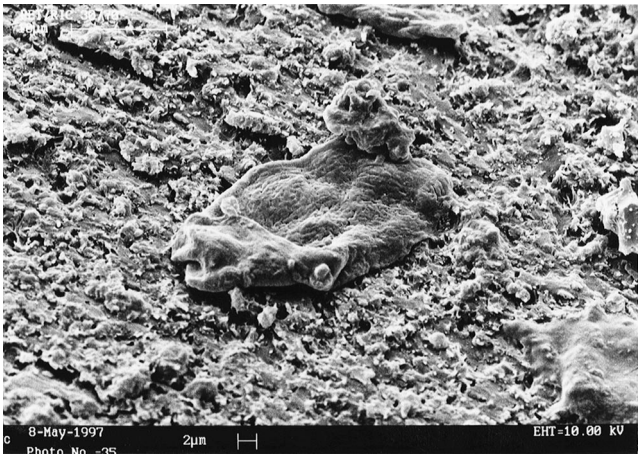

Fig. 7. Micrograph of the PET/**P2** 30/70 w/w blend, showing a large island of PET in a matrix of **P2**.

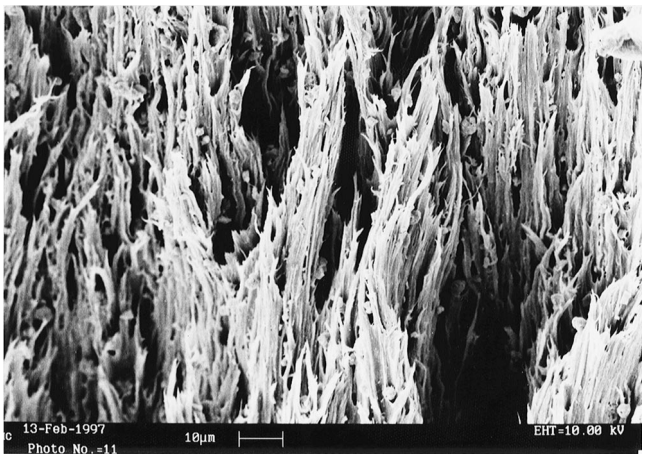

Fig. 8. Micrograph of the PET/**P2** 80/20 w/w blend after tensile fracture. Note the strong adhesion of LCP droplets to strained PET filaments.

that is easier to identify with respect to the analogous blend of PET with **P1**.

Blends containing **P2** were observed also after tensile tests leading to fracture. Strong adhesion between the two polymers is testified by droplets of **P2** still remaining attached to strained PET in a specimen containing 20% LCP (Fig. 8). This can explain the reinforcing action of the random polymer on PET; at the same time, the globular morphology of the dispersed phase confirms that the reinforcing agent is particle-like. It is interesting to remark that the highest increases in modulus are reported for samples with a low **P2** content, where some evidence of fibrillar morphology is present.

Finally, it could be observed that when the fracture behaviour began to change from ductile to fragile (70/30 composition), the fragile islands of **P2** were embedded in ductile PET and sometimes could stop the crack propagation [Fig. 9(A)], whereas in other situations the break was sudden [Fig. 9(B)].

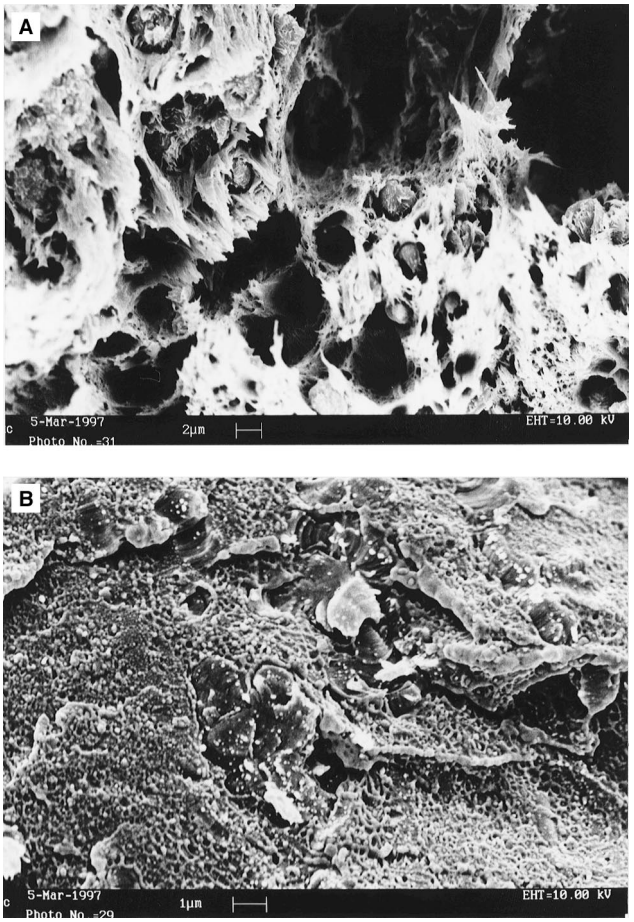

Fig. 9. Micrographs of PET/**P2** 70/30 w/w blends after tensile fracture: (A) ductile fracture; (B) fragile fracture.

4. Concluding remarks

All of the techniques used gave relevant information on the binary systems under study, with the exception of d.m.t.a. The latter technique proved that **P1** is not or slightly miscible with PET, but did not provide much further insight on the possible partial miscibility of **P2** and PET because their glass transitions are too close.

The study of these two polymer blends revealed a number of interesting topics that will be the subject of following work. In particular it should be determined whether the presence of a catalyst or an inhibitor, together with longer processing times at high temperature, can produce some detectable change in the thermal behaviour and/or morphological aspect of the blends. This could support some interpretations in the present paper for which we could not find direct proof, such as the occurrence of ester-exchange reactions in the molten blend and their possible influence on the crystallization process of PET. At the same time, the study of blends with high **P2** content could also reveal the occurrence of a 'register-induced' effect in the liquid-crystal component of block copolymers which can so positively affect the overall crystallinity.

Moreover, preliminary results on other nematic polymers similar to those studied here seem to indicate that the modulus of PET can be doubled while still maintaining good ductility. This encourages further work on these blends, in view of the considerations reported in the introduction of this paper.

References

[1] La Mantia FP, editor. Thermotropic liquid crystal polymer blends. Lancaster, PA: Technomic, 1993.
[2] Brostow W. Kunstsoffe 1988;78:411.
[3] Brostow W. Polymer 1990;31:979.
[4] Brostow W. In: Collyer AA, editor. Liquid crystalline polymers: from structures to applications. London: Elsevier Applied Science, 1992:Ch. 1.
[5] Brostow W, Sterzynski T, Triouleyre S. Polymer 1996;37:1561.
[6] Brostow W, Hess M, Lopez BL, Sterzynski T. Polymer 1996;37:1551.
[7] Utracki LA. Polym Eng Sci 1983;23 (11):602.

[8] Han CD, Kim YM, Chen SJ. J Appl Polym Sci 1975;19:2381.
[9] Blizard KG, Baird DG. Polym Eng Sci 1987;27:653.
[10] Beery D, Kenig S, Siegmann A. Polym Eng Sci 1991;31:451.
[11] Beery D, Kenig S, Siegmann A. Polym Eng Sci 1991;31:459.
[12] Perkins WG, Marcelli AM, Frerking HW Jr. J Appl Polym Sci 1991;43:329.
[13] Silverstein MS, Hiltner A, Baer E. J Appl Polym Sci 1991;43:157.
[14] Datta A, Chen HH, Baird DG. Polymer 1993;34:759.
[15] Heino MT, Seppälä J. J Appl Polym Sci 1993;48:1677.
[16] Griffin BP, Cox MK. Br Polym J 1980;12:147.
[17] Irwin RS, Sweeny W, Gardner KH, Gochanour CR, Weinberg M. Macromolecules 1989;22:1065.
[18] Skovby MH, Heilmann CA, Kops J. In: Weiss RA, Ober CK, editors. Liquid crystalline polymers (ACS Symposium Series vol. 435). Washington, DC: American Chemical Society, 1990.
[19] Kricheldorf HR, Döring V, Schwarz G. J Polym Chem 1990;75:28.
[20] Carpaneto L, Costa G, Marsano E, Valenti B, Guenza M. Polym Adv Technol 1992;4:367.
[21] Carpaneto L, Costa G, Marsano E, Morinelli S, Piombo V, Valenti B. Polym Adv Technol 1993;5:416.
[22] Carpaneto L, Costa G, Peluffo C, Vezzani S, Valenti B. Macromol Chem Phys 1996;197:1669.
[23] Carpaneto L, Peluffo C, Piaggio P, Valenti B. Faraday Trans 1997;93 (6):1095.
[24] Bacon RGR, Hill HAO. J Chem Soc 1964:1097.
[25] Bacon RGR, Hill HAO. J Chem Soc 1964:1108.
[26] Higashi F, Yamada Y, Hoshio A. J Polym Sci, Polym Chem Edn 1984;22:2181.